

EFFECT OF MOLECULAR WEIGHT ON CAPILLARY ABSORPTION OF POLYMER DROPLETS

Gerald G. PEREIRA^{1*} and Srikanth DHONDI

¹CSIRO Mathematics, Informatics and Statistics, Clayton, Victoria 3169, AUSTRALIA

*Corresponding author, E-mail address: Gerald.Pereira@csiro.au

ABSTRACT

We study capillary absorption of small polymer droplets into non-wettable capillaries using coarse-grained molecular dynamics simulations and simple analytic models. We study the effect of polymer chain length on the capillary absorption process. Our simulations reveal that for droplets of the same size (radius), the critical tube radius, below which there is no absorption, increases with the length of the polymer chains that constitute the droplets. We propose a model to explain this effect, which incorporates an entropic penalty for polymer confinement and find that the model agrees quantitatively with the simulations. We also find that the absorption dynamics is sensitive to the polymer chain length.

NOMENCLATURE

σ characteristic length
 ε characteristic energy
 τ characteristic time
 N polymer chain length

INTRODUCTION

Capillary action has a wide range of applications in nature and industry (Marmur, 1988, Zhmud et al, 2000). This phenomenon, in general, is very well understood at the macroscopic scale. However, the standard macroscopic models on capillarity make certain assumptions that may not be always valid (Marmur, 1988). One particular assumption which holds importance in the context of micro/nanofluidics is the size of the liquid reservoir (Marmur, 1988, 1992). Standard macroscopic models assume that the liquid reservoir is infinite compared to the tube dimensions. However, in many micro/nanofluidic systems the size of the liquid reservoir is often comparable to the device dimensions. Thus, in such situations, to describe the system behaviour correctly finite size effects need to be taken into account.

Marmur (1988) first studied the effect of finite size of liquids on the statics and dynamics of capillarity. He argued that the Laplace pressure originating from the curvature of the droplets should play an important role in determining the underlying capillary process. As the system size is scaled down these finite size effects become ever more important, which could give rise to novel behaviour that are absent otherwise. For example, it was found that capillary absorption of non-wetting liquids is possible if the droplets are sufficiently small (Ajayan and Iijima, 1993, Schebarchov and Henty, 2008). This is in

contrast with the macroscopic theories, according to which there should be no capillary action for non-wetting liquids (contact angles greater than 90°).

There is a growing interest in building polymer-based functional nanomaterials and nanostructures for novel applications. One of the methods used for producing these nanostructures is by filling nanomolds with the aid of capillary forces. For example, polymer-based nanopatterned wires (Zhang et al, 2002), nanorods and nanotubes (Zhang et al, 2006), nanoscale protein patterning, nanofibers (Pisignano et al, 2005), nanobelts (He et al, 2007), etc. were produced using capillary forces. Most of these methods fall in the above described regime, that is the size of the liquid reservoir is finite compared to the channel/tube dimensions. Thus, in these situations, the Laplace pressure driven capillary forces can become important.

Compared to Newtonian fluids, the behavior of polymer solutions or melts at the nanoscale is particularly fascinating because at these dimensions the characteristic length scales of polymers become comparable to the device dimensions. This can have important implications on the behavior of polymers in these devices and can lead to new phenomena. In the context of nanocapillaries, the question that received most attention, recently, is whether the Lucas-Washburn equation (Lucas, 1918, Washburn, 1921) for capillary rise applies at the nanoscale (Schebarchov, 2008). This is yet to be fully resolved, with the literature containing conflicting results (Zhmud et al, 2000 and references therein).

Capillary phenomena of polymer liquids at the nanoscale can be expected to be different from their Newtonian counterparts because of their molecular nature. When a polymer molecule is forced to enter a tube whose diameter is comparable to its size then the molecule has to stretch in the direction of the tube. This results in a conformational entropy loss. Therefore, in the case of polymer droplets for absorption to take place the Laplace pressure must overcome the conformational entropy loss in addition to the meniscus pressure. Furthermore, the entanglement effects may play an important role in influencing the underlying capillary process. Entangled polymers are known to display two different dynamics regimes depending on their chain lengths. Melts with shorter chains exhibit Rouse-type dynamics whereas those with longer chains showcase reptation-type dynamics (deGennes, 1979).

Keeping in view the above arguments the capillary phenomena of polymer droplets at small scales has the potential to display different behaviour to their Newtonian counterparts. Therefore, it is of considerable interest to study the effect of molecular size on the thermodynamics and dynamics of polymer droplets under capillary action. For this purpose, we carry out molecular dynamics (MD) simulations of polymer droplets of same size but composed of different chain lengths, N . We restrict our simulations to the two cases, $N=20$ and 200 , as the former falls in the Rouse regime and the latter falls in the reptation regime. From this we should be able to observe any noticeable differences in the capillary dynamics. The simulation results will then be compared against a simple analytical model.

MODEL DESCRIPTION

The method we use to simulate polymer absorption is MD and full details are given in a recent work of ours (Dhondi et al, 2012). Here we give a brief overview of the simulation method. The polymer molecules were modelled as coarse grained bead-spring chains where each chain consisted of N -effective monomers. The interaction between bonded monomers was given by the finite extensible nonlinear elastic (FENE) potential, which is Gaussian for small separations and much stiffer at larger separations. The excluded volume and attractive interactions between non-bonded monomers and between the monomers and substrate/tube atoms were included via the shifted Lennard-Jones (LJ) 12-6 potential (Dhondi et al, 2012). The length and energy scales in the LJ units are given by σ and ϵ respectively (and for convenience both are set to unity). All units are then expressed in terms of these quantities.

The time integration of the equations of motion was carried out using the velocity Verlet algorithm. During this equilibration period the LJ potential between monomers was turned-off to prevent unrealistically large forces. The temperature of the system was controlled at $T = \epsilon/k_B$ using the Langevin thermostat and the corresponding equation of motion for any particle i is given by

$$m \frac{d^2 \vec{r}_i}{dt^2} + m \Gamma \frac{d \vec{r}_i}{dt} = - \sum_{j \neq i} \vec{F}_{ij} + f_i \quad (1)$$

where m is a monomer mass, Γ is a friction constant, f_i is the random force (mimicking thermal fluctuations) applied on monomer i and $\vec{F}_{ij} = -\nabla U_{ij}$ is the total force experienced by particle i due to its interaction with particle j . The time scale is given by $\tau \equiv (m\sigma^2/\epsilon)^{1/2}$.

CHARACTERIZATION OF THE DROPLET

Properties of the droplets, which are of interest to our study, were extracted by recording their configurations every 100τ for 50000τ . First of all we calculate the radius of droplets made up of chains of different length but consisting of the same number of total monomers. (For example, for a droplet of 8000 monomers we ran separate simulations of 400 chains of length 20, 80 chains of length of 100 and so on.) The average droplet radius $\langle R_0 \rangle = 15.03 \pm 0.07\sigma$ for droplets with 8000 monomers and $\langle R_0 \rangle = 18.58 \pm 0.07\sigma$ for droplets with 16000

monomers (where the error represents the standard deviation computed over all considered chain lengths). The narrow distribution in droplet radius indicates that there is very little effect of chain length on the droplet size. This is useful to know since we want to study the capillary action of droplets of same size but made up of chains of different lengths.

For droplets of same size, the local environment experienced by an average chain should change with chain length, N . To investigate this effect we calculate the average radius of gyration per chain as a function of N . In the small N limit on average chains behave as if they were ideal chains, i.e. their radius of gyration scales as $\langle R_g \rangle \propto N^{1/2}$. There appears to be a cross-over from this behavior for $N > 200$. A possible explanation for this trend may be as follows. In small N droplets, on average, each chain is surrounded by a large number of chains, equally in all directions. This is analogous to a chain in a melt, which is ideal. As N increases on average each chain will have fewer polymer neighbours, i.e. more exposure to solvent. Hence the trend in $\langle R_g \rangle$ deviates from the ideal chain behaviour. These results were then compared against single chain simulations, conducted under the same conditions as the droplet simulations above. The single chain simulations reveal that the chains display poor solvent behaviour, where $\langle R_g \rangle \propto N^{1/3}$. In the limit N approaching the system size (total number of monomers in the droplet), the curve from the droplet simulations converges onto the single chain curve. This observation supports our earlier explanation for the shrinkage in $\langle R_g \rangle$ for droplets with larger N values (de Gennes, 1979). Similar $\langle R_g \rangle$ behaviour was observed for larger droplets of 16000 monomers.

Contact Angle Measurements

The contact angle, θ , between the liquid and solid can be used to discriminate between wetting and non-wetting surfaces. Within the framework of MD simulations control over the contact angle can be gained by tuning the interaction between the liquid and solid constituents. By varying the strength of this interaction the wetting properties of the liquid with respect to the solid can be changed.

Equilibrated polymer droplets were placed on a single atom thick, simple cubic substrate with a lattice constant σ . The substrate atoms were fixed in space to reduce the computational effort. Although, in reality, the substrate atoms vibrate about their equilibrium positions, this should not influence the nature of the results since all the simulations were conducted under the same condition (stationary substrate atoms). The interaction between the substrate atoms and monomers was given by the LJ potential.

In the case of wetting droplets the chains can crawl on the outer side of the tube. Moreover, wetting liquids are found to have a precursor foot spreading ahead of the liquid bulk thus making the contact angle time-dependent (deGennes, 1979). For these two reasons we restrict ourselves only to

non-wetting droplets. We adjusted the LJ potentials to ensure these conditions.

Contact angles were extracted by approximating the equilibrated droplet, on the substrate, to a spherical cap. If a droplet with an initial radius r_0 assumes a spherical cap geometry, of height h , upon reaching equilibrium then the contact angle formed by the spherical cap is

$$\theta_c = \cos^{-1} \left(1 - \frac{3}{4r_0^3/h^3 + 1} \right). \quad (2)$$

In our simulations, the droplets were initially equilibrated for 10000τ on the substrate to let them reach their equilibrium state (height). After this time period, we noted the droplet configurations every 100τ for the next 40000τ to calculate the average height $\langle h \rangle$ of the spherical cap.

The average radius of the droplet $\langle r_0 \rangle$ are available from the previous section. By solving Eq. (2) we can approximate θ_c . The contact angle remains approximately constant independent of the chain length or the droplet size, within the studied chain length range. We estimate the average contact angle for, this case, as $\theta_c = 104^\circ$ within 1% error.

CAPILLARY ABSORPTION OF POLYMER DROPLETS

In the context of non-wetting polymer droplets, for capillary absorption to take place, the Laplace pressure must overcome conformational entropy loss in addition to meniscus pressure. It is also worthwhile to consider the dynamics of the underlying process. As mentioned earlier, the validity of the Lucas-Washburn equation at the nanoscale is debatable. We suspect entanglement effects will play a role in determining the dynamics at nanoscale. Entangled polymers are known to display different dynamic regimes depending on their chain lengths. Melts with shorter chains exhibit Rouse-type dynamics whereas those composed of longer chains showcase reptation-type dynamics (deGennes, 1979). Therefore, it is of considerable interest to study the effect of molecular size on the statics and dynamics of polymer droplets under capillary action. For this purpose, we carry out MD simulations of polymer droplets of the same size (total number of monomers is constant) but composed of different chain lengths. We restrict our simulations to two cases, $N = 20$ and 200 as the former falls in the Rouse regime and the latter falls in the reptation region. This difference in chain dynamics should capture any significant differences in the observed capillary absorption dynamics.

The tube was constructed by rolling a single atom thick, simple cubic layer with a lattice constant 1.0σ into a cylinder with both ends of the tube being open. The tube atoms remained fixed. An equilibrated droplet was placed at the entrance of one of the ends of the tube (see Fig. 1). The equations of motion were integrated via the velocity Verlet algorithm with a time-step of 0.01τ .

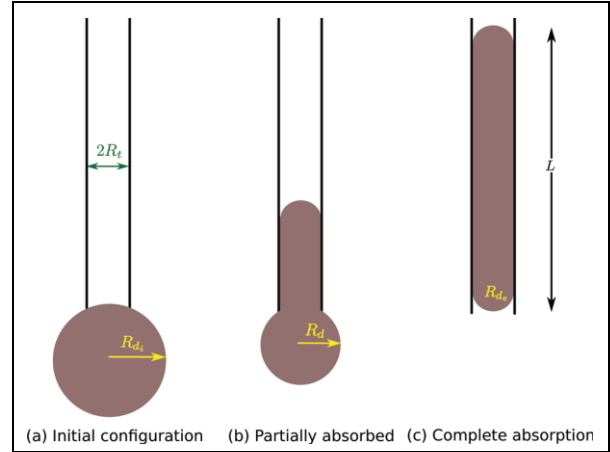


Figure 1: Schematic diagram of geometry

Droplets with 8000 Monomers

We first report the results for an 8000 monomer droplet and later compare them with the results for a larger droplet with 16000 monomers. For a droplet of fixed size, the tube radius was varied systematically to determine the critical tube radius, r_{tc} , below which no absorption takes place. A number of simulations were run for different tube radii ranging from 4.26σ to 6.69σ and the subsequent absorption process was monitored for each of the cases. From these simulations we were able to narrow down the critical tube radius region and here we only focus on results from this region. The absorption process was monitored by recording the height of the protruding liquid meniscus inside the tube and the radius of the protruding droplet as a function of time. The results for $N = 20$ case are shown in Fig. 2. For a smaller tube radius of $r_t = 5.10\sigma$, the radius of the protruding droplet and height of the liquid meniscus does not change over time. But for a slightly larger radius of $r_t = 5.26\sigma$ the droplet gets absorbed into the tube, once the system overcomes the initial energy barrier for penetration. Corresponding to the capillary absorption, the height of the meniscus increases and the radius of the protruding droplet decreases.

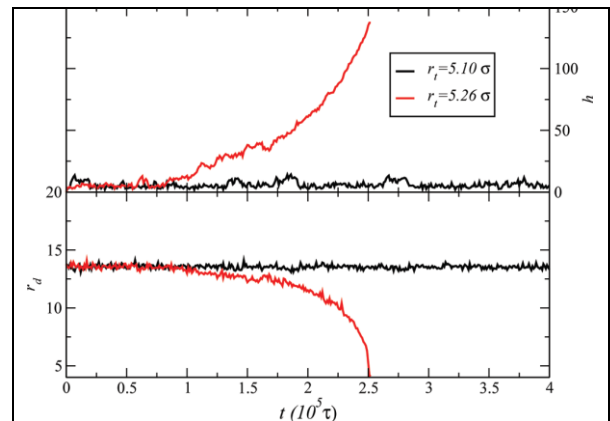


Figure 2: Meniscus height and the radius of protruding droplet as a function of time for 8000 monomers with $N=20$, for different tube radii.

In order to determine the critical cut-off radius below which there is no absorption, the simulation with smaller

tube radius of $r_t = 5.10\sigma$ was run for much longer. Yet there was no absorption indicating the critical radius is 5.26σ (for $N=20$). To test the applicability of the Lucas-Washburn description to our systems we fit the meniscus height data to (Washburn, 1921):

$$h(t) = \left(\frac{\gamma(R_d(t) + 4b) \cos \theta_c}{2\mu} \right) t^{1/2}, \quad (3)$$

where γ is the surface tension, R_d is the radius of the protruding droplet at time t , b is the slip length, and μ is the viscosity of the fluid. The initial portion of the meniscus height data were ignored as the Lucas-Washburn description does not account for inertial forces at initial time. The fit to the meniscus height for $r_t = 5.26\sigma$ was found to be in poor agreement with Eq. 3 (see Fig. 3).

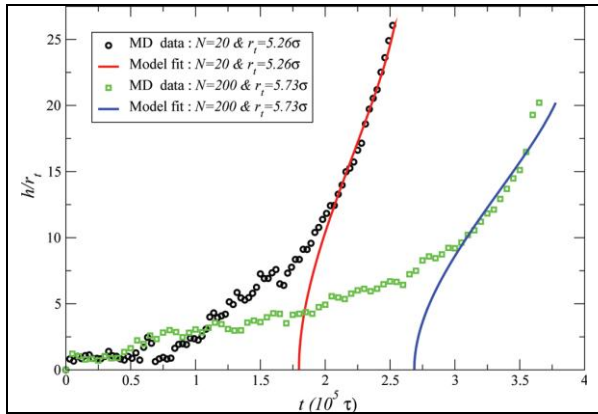


Figure 3: The data points indicate the MD simulation results while the solid curves are model fits to Eq. (3), for two different cases and chain lengths. The model at most describes very late stage dynamics.

Similar calculations were carried out for an 8000 monomer droplet made up of $N = 200$ chains, to examine the effect of molecular size on the whole process. The meniscus height and the radius of the protruding droplet for this case are plotted in Fig. (4). Several interesting outcomes can be observed from this plot. For tubes smaller than $r_t = 5.57\sigma$ there was no absorption, within the time scale of the simulation runs. The absorption process was almost spontaneous for the case of $r_t = 5.73\sigma$ barring the initial times. The most interesting case of all was $r_t = 5.57\sigma$ where the droplet sits outside the tube entrance for a very long time, during which the droplet tries to enter the tube by overcoming some sort of barrier. This is clearly evident from the meniscus height plot. The origin of this barrier can be energetic or entropic, due to conformational entropy loss, or a combination of both. During this period, we also observe partial absorption and desorption taking place. Such a process was neither present in the $N = 20$ case nor was reported earlier for either Newtonian or non-Newtonian fluids. Eventually, the droplet overcomes this barrier and gets drawn up the tube. We attribute this effect to the increase in molecular size, N . The average behaviour of chain size for this case is shown in Fig. 5. Prior to absorption, while the droplet attempts to enter the tube, fluctuations in the y -component of the radius of gyration were observed and the trend in

these fluctuations coincides with the partial absorption and desorption in the meniscus height (see Fig. 5). (Note the tube axis is aligned with the y -axis.)

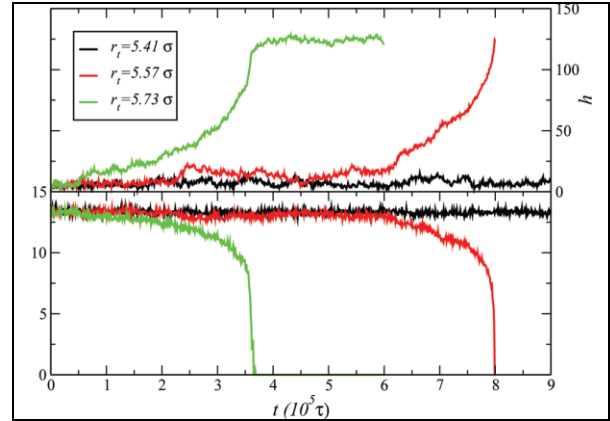


Figure 4: Meniscus height and radius of protruding droplet as function of time for $N=200$, for different tube radii.

Because of the partial absorption and desorption processes, there was either an increase or decrease in the y -component of radius of gyration, corresponding to a compression or expansion of the other two components observed. Hence the average behaviour of the components of radius of gyration is a good measure of the underlying phenomena. Another interesting observation from this simulation was the capillary dynamics. Once again we found that the capillary dynamics observed here cannot be described by the Lucas-Washburn description (Eq. 3). Moreover, the standard capillary models cannot explain the process of partial absorption and desorption observed in this case. The average chain size measurements were also performed on the bigger tube radius $r_t = 5.73\sigma$ case.

In this particular case, we were able to study the system behaviour after complete absorption, mainly due to faster dynamics involved compared to the previous case of $r_t = 5.57\sigma$. Once the droplet was totally absorbed into the tube, the meniscus height remained approximately constant (see Fig. 4), during which period we monitored the average radius of gyration components. An interesting observation from this calculation was that after complete absorption the chains started to relax. In the long time limit, we expect the chains to retain their original size in the bulk (unless obstructed by the capillary walls).

Droplets with 16000 Monomers

Absorption simulations were also performed for larger droplets with 16000 monomers for chain lengths 20 and 200. The critical tube radius region was identified by conducting a number of simulations for r_t between 4.94σ and 7.49σ . Apart from the fact that larger droplets require broader tubes for absorption, which stems from Marmur's theory, we also noticed some other interesting physics related to absorption dynamics. We shall report them one by one here. First, we present results for absorption of an $N = 20$ droplet. The height of the meniscus and radius of the protruding droplet are presented in Fig. 6 showing the critical tube radius is 6.37σ . The activation time, time after which the absorption process starts, has increased considerably compared to the 8000 monomer droplet for

the same chain length. This could be due to an increase in curvature of the droplets resulting in weaker Laplace forces.

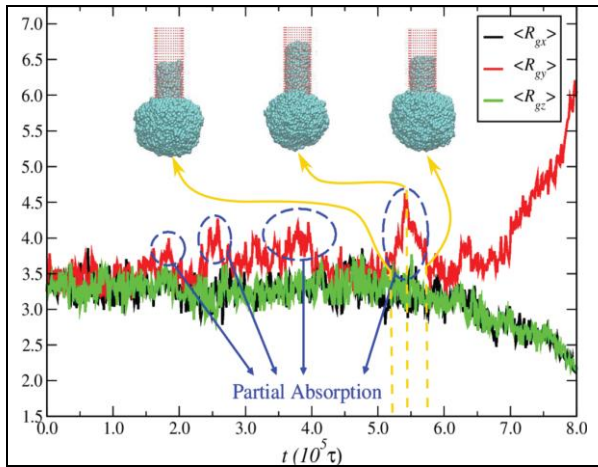


Figure 5: Components of the radius of gyration for tube radius 5.57σ , for $N=200$ and 8000 monomers in total. The blue dashed encircled regions show the partial absorption instances (which are demonstrated with the help of snapshots).

Results for $N = 200$ droplets show remarkably different behaviour in comparison with any of the earlier cases presented. The meniscus height plots are sufficient to bring about this contrast and trends in the radius of the protruding droplet, R_g , and potential energy calculations complement its findings. The meniscus height plots for different r_t are shown in Fig. 7 and the critical tube radius is 6.69σ . In the case of $r_t = 6.53\sigma$ throughout the simulation period the droplet was found to partially absorb and desorb without ever being able to cross the barrier.

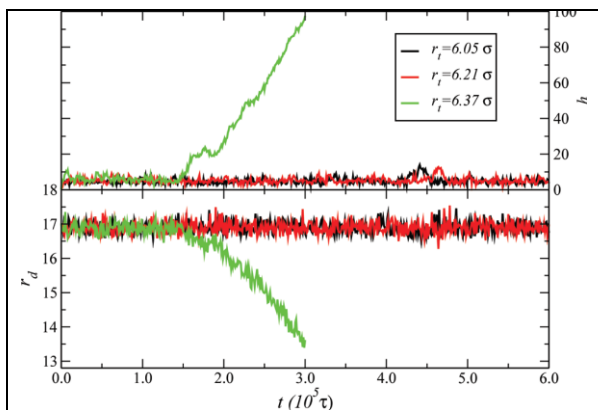


Figure 6: Meniscus height and radius of protruding droplet plots for the 16000 monomer droplet with $N=20$, for various tube radii.

One can argue that this is purely a dynamic issue, given long enough time the droplet may eventually overcome this barrier with the help of fluctuations and capillarity phenomenon can be observed. Though we do not deny this possibility, it is not at the core of our claims, which is the precise identification of the critical tube radius. The most interesting observation was the persistent partial absorption and desorption of the droplet, which has not

been reported before. For a slightly larger tube of $r_t = 6.69\sigma$, the droplet gets stuck in multiple metastable states, for long periods of times. This scenario implies that the droplet is partially inside and partially outside for relatively long time periods. Such a process contrasts with existing dynamic theories aimed at explaining the capillary dynamics of simple liquids.

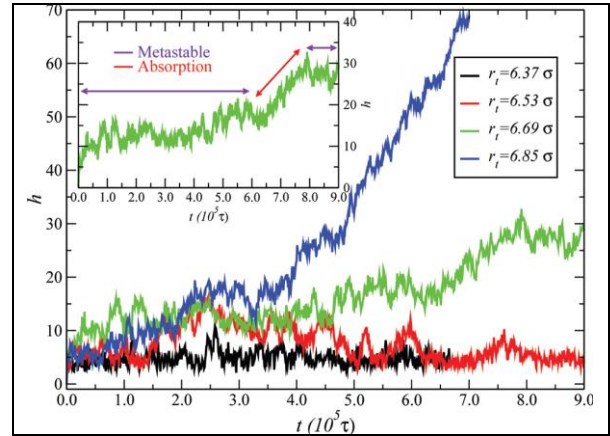


Figure 7: Meniscus height of protruding droplet plots for the 16000 monomer droplet with $N=200$, for various tube radii. In the inset we highlight the metastable and partial absorption regions for the case of $r_t = 6.69\sigma$.

Comparison with theory

The MD results from the previous sections show for droplets composed of longer chains, a larger critical tube radius is required than for droplets composed of shorter chains. Specifically, we have found that the radius of gyration of the $N=20$ chains is 2.14σ while the $N=200$ chain is 5.83σ , compared to critical tube radii of roughly 5.26σ and 5.57σ (respectively) for the droplet composed of 8000 monomers and 6.37σ and 6.69σ (respectively) for the droplet composed of 16000 monomers. We shall now attempt to understand the previous MD simulation results from a theoretical point of view - why do the droplets composed of longer chains have a larger critical tube radius? We only consider equilibrium thermodynamics here and therefore only model the initial and final, equilibrium conformations of the polymer droplets (Fig 1a and 1c). Previously Schebarchov and Hendy (2008) were able to show that non-wetting metallic droplets could be drawn up a narrow capillary tube if the droplet radius was sufficiently small. Their theoretical analysis was based on surface tension arguments (between the metallic droplet, the tube walls and the surrounding solvent) which gives rise to a Laplace pressure which assists the droplet in rising up the tube. Our analysis is based on these ideas, however, the complicating factor is that for polymer chains one needs to account for chain entropy. If a chain is confined within a narrow tube the number of possible conformations it may investigate decreases and as a result the chain's free energy increases.

We don't go through all the details here as they are given elsewhere (Dhondi et al, 2012), but only an overview. Figure 1a shows a polymer droplet before entering the tube. We can readily calculate its surface energy (proportional to surface area) and there is no penalty in

chain conformational entropy (as all polymer chains are random walk chains). We call this configuration I . If the polymer droplet is absorbed in the tube it takes up a configuration shown in Fig. 1c. The surface energy is easily calculated but the entropy penalty now is more difficult. Chains are perturbed from their random walk configuration by the presence of the capillary walls. Every time a polymer chain hits a capillary wall it experiences an energy penalty of $k_B T$. We can then calculate the energy for a polymer droplet consisting of q chains of length N , where for a particular set of simulations we kept qN constant (at 8000 or 16000). The conformational entropy penalty is

$$\Phi_{II}^P = qk_B T \left(N \frac{b^2}{r_t^2} - 1 \right), \quad (4)$$

Where b is a random walk step length and r_t is the tube radius. The subscript II indicates this is for configuration II (Fig. 1c).

Configuration II is favoured if it has a lower free energy compared to configuration I . We thus define the difference in free energy between the two configurations, $\Delta\Phi \equiv \Phi_{II} - \Phi_I$. It is given by

$$\Delta\Phi = \frac{1}{3\eta} \left(\frac{1}{1 + \sin \theta_c} + \sin \theta_c \right) - \frac{2}{3} \eta \cos \theta_c - 1 + \frac{\eta}{3\kappa(r_d/r_t)}, \quad (5)$$

where $\eta \equiv r_d/r_t$ and $\kappa \equiv \gamma b^2/k_B T$. The absorbed state is favoured when $\Delta\Phi < 0$.

Figure 8 shows the free energy for a contact angle of 103.5 degrees. (Recall the contact angle from the MD simulations was in the non-wetting regime ($\approx 103.5^\circ$)). In the absence of the polymeric term, all droplets below a radius of $6.35 r_t$ would be absorbed into the capillary. For both polymeric cases, however the critical tube radius is smaller (at $5.5 r_t$ for the 1000 length chains and $5.3 r_t$ for the million length chain) and the critical η decreases with increasing chain length. In our MD simulations for the droplet of 8000 monomers, the critical η for short chains ($N=20$) is 2.9, which for longer chains ($N=200$) is 2.7. For the droplet of 16000 monomers, the critical η for short chains ($N=20$) is 2.95, while for longer chains ($N=200$) is 2.8. Thus the theoretical results agree with our MD simulations qualitatively in that both MD simulations and theory predict (i) a decrease in critical η with longer chains and (ii) when a simple molecular fluid droplet would be absorbed, the polymeric droplet remains outside the tube. This difference can only be attributed to the entropy penalty the chains must overcome when entering a restricted domain.

CONCLUSION

The results of both MD and equilibrium statistical mechanics theory indicates droplets composed of longer polymer chains find it more difficult to absorb into a narrow, non-wetting capillary than droplets composed of shorter chains. We have shown this is due to the entropical

(conformational) energetic penalty which affects longer chains more drastically than shorter chains. These results will have important implications on any micro or nano-fluidic applications involving polymer droplets such as producing nanowires, nanofibres or nanorods.

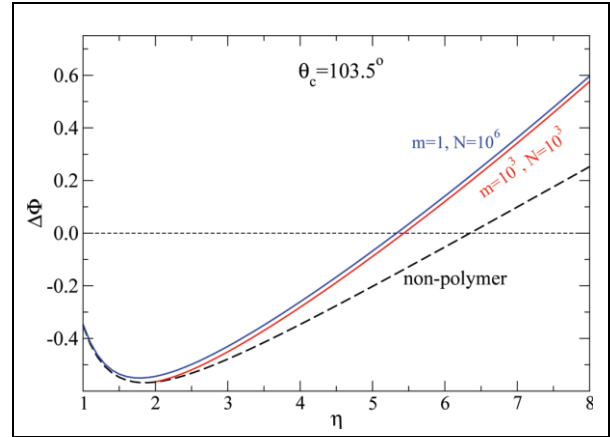


Figure 8: Free energy for various droplet configurations at $\theta_c = 103.5^\circ$ for various η .

REFERENCES

- AJAYAN, P.M., and IIJIMA, S., (1993), "Opening carbon nanotubes with oxygen and implications for filling", *Nature*, **361**, 333-334.
- DE GENNES, (1979), "Scaling concepts in polymer physics", *Cornell Uni Press: London*.
- DHONDI, S., PEREIRA, G.G. and HENDY, S.C., (2012), "Effect of molecular weight on the capillary absorption of polymer droplets", *Langmuir*, in press.
- HE, D., WU, Y., XU, B.Q., (2007), "Formation of 2, 3-diaminophenazines and their self-assembly into nanobelts in aqueous media", *Eur. Polym. J.*, **43**, 3703-3709.
- LUCAS, R., (1918), "The time law of capillary rise of liquids", *Kolloid Z.*, **23**, 15-22.
- MARMUR, A., (1988), "Penetration of a small drop into a capillary", *J. Colloid Interface Sci.*, **122**, 209-219.
- MARMUR, A., (1992), "Penetration and displacement in capillary systems of limited size", *Adv. Colloid Interface Sci.*, **39**, 13-33.
- PISIGNANO, D., MARUCCI, G., MELE, E., PERSANO, L., BENEDETTO, F.D. and CINGOLANI, R., (2005), "Polymer nanofibres by soft lithography", *Appl. Phys. Lett.*, **87**, 123109(1-3).
- SCHEBARCHOV, D., and HENDY, S.C., (2008), "Capillary absorption of metal nanodroplets by single walled carbon nanotubes", *Nano Lett.*, **8**, 2253-2257.
- WASHBURN, E.W., (1921), "The dynamics of capillary flow", *Phys. Rev.*, **17**, 273-283.
- ZHANG, F., NYBERG, T., and INGANAS, O., (2002), "Conducting polymer nanowires and nanodots made with soft lithography", **2**, 1373-1377.
- ZHANG, M., DOBRIYAL, P., CHEN, J.-T., RUSSELL, T.P., (2006), "Wetting transition in cylindrical alumina nanopores with polymer melts", *Nano Lett.*, **6**, 1075-1079.
- ZHMUD B.V., TIBERG F., and HALLSTENSON K., (2000), "Dynamics of capillary rise", *J. Colloid Interface Sci.*, **228**, 263-269.